CrossMark

RESEARCH ARTICLE

Sediment cores from kettle holes in NE Germany reveal recent impacts of agriculture

Andreas Kleeberg[1,4] · Marielle Neyen[1,2] · Uwe-Karsten Schkade[3] · Thomas Kalettka[1] ·
Gunnar Lischeid[1]

Abstract Glacial kettle holes in young moraine regions receive abundant terrigenous material from their closed catchments. Core chronology and sediment accumulation were determined for two semi-permanent kettle holes, designated RG and KR, on arable land close to the villages of Rittgarten and Kraatz, respectively, in Uckermark, NE Germany. Core dating (^{210}Pb, ^{137}Cs) revealed variable sediment accretion rates through time (RG 0.4–23.1 mm a^{-1}; KR 0.2–35.5 mm a^{-1}), with periods of high accumulation corresponding to periods of intensive agricultural activity and consequent erosional inputs from catchments. Sediment composition (C, N, P, S, K, Ca, Fe, Mn, Zn, Cu, Mo, Pb, Cd, Zr) was used to determine sediment source and input processes. At RG, annual P input increased from 0.65 kg ha^{-1} in the early nineteenth century to 1.67 kg ha^{-1} by 2013. At KR, P input increased from 0.6 to 4.1 kg ha^{-1} over the last century. There was a concurrent increase in Fe input in both water bodies. Thus, Fe/P ratios showed no temporal trend and did not differ between RG (18.5) and KR (18.4), indicating similar P mobility. At RG, the S/Fe ratio increased from 0.4 to 2.3, indicating more iron sulphides and thus higher P availability, coinciding with high coverage of duckweed (*Spirodela polyrhiza* (L.)) and soft hornwort (*Ceratophyllum submersum* L.). At KR, however, this ratio remained low and relatively unchanged (0.3 ± 0.4), indicating more efficient Fe-P binding and lower hydrophyte productivity. Trends in sediment composition indicate a shift towards eutrophication in both kettle holes, but with differences in timing and magnitude. Other morphologically similar kettle holes in NE Germany that are prone to erosion could have been similarly impacted but may differ in the extent of sediment infilling and degradation of their ecological functions.

Keywords Depressional wetlands · Agriculture · Sediment accretion · Radioisotopic dating · Metals · Phosphorus · Eutrophication history

✉ Andreas Kleeberg
 Andreas.Kleeberg@landeslabor-bbb.de

1 Leibniz Centre for Agricultural Landscape Research, Institute of Landscape Hydrology, Eberswalder Straße 84, 15374 Müncheberg, Germany

2 Present address: Present address: Department Geosciences, Institute of Geographical Sciences, Freie Universität Berlin, Malteserstr. 74-100, 12249 Berlin, Germany

3 Federal Office for Radiation Protection, Köpenicker Allee 120, 10318 Berlin, Germany

4 Present address: Present address: Department Geology, Soil, Waste, State Laboratory Berlin-Brandenburg, Stahnsdorfer Damm 77, 14532 Kleinmachnow, Germany

Introduction

Sediment deposition in lakes is controlled mainly by climate, geology and land cover in the catchment, basin morphology, tributaries, hydrodynamics, and productivity (Engstrom et al. 2006; Gąsiorowski 2008). Some of these factors can be directly or indirectly influenced by human activities (Karasiewicz et al. 2014). Thus, rapid changes in sedimentation rate and nutrient input, detected in lake sediment cores, often reflect local historical events such as residential development, land use change, or even war (Battarbee et al. 2005; Rose et al. 2011). Net sediment accretion in lakes is also influenced by aquatic plant and animal communities (Engstrom et al. 2006).

Few paleolimnological studies linking sedimentation characteristics and human activities have been conducted in small

inland water bodies such as ponds (Verstraeten and Poesen 2002; Kleeberg et al. 2010), morainic depressional wetlands, so-called prairie potholes (Preston et al. 2013) or kettle holes (Frielinghaus and Vahrson 1998; Lamentowicz et al. 2008; Karasiewicz et al. 2014). Kettle holes are typically located in hummocky lowland areas that are used for agriculture and other human activities (Kalettka and Rudat 2006; Karasiewicz et al. 2014). Whereas large water bodies receive low amounts of terrestrial material relative to their volume (Carignan et al. 2000; Biddanda and Cotner 2002), small water bodies receive relatively much more terrigenous material, which originates in the catchment (Molot and Dillon 1996; Biddanda and Cotner 2002). As such, kettle holes probably receive substantial inputs of non-point-source agricultural pollution and eroded soil from their closed watersheds (Frielinghaus and Vahrson 1998; Havens et al. 2007). Thus, their sediments are sinks for nutrients such as phosphorus (P), as well as metals and other pollutants (Bilotta et al. 2007). Increased sedimentation and altered nutrient cycles associated with agriculture threaten both the permanence and ecological functionality of these resources (Pienkowski 2000; Kalettka et al. 2001; Preston et al. 2013).

Because site conditions differ among the kettle holes, the region Uckermark is a hotspot for biodiversity of endangered amphibian species (Berger et al. 2011), large branchiopods (Gołdyn et al. 2012) and aquatic macrophytes (Pätzig et al. 2012; Altenfelder et al. 2014). Drainage, fertilization and herbicide use in surrounding arable fields during the past few decades, however, has led to a severe decline in diversity of both plant species (Altenfelder et al. 2014) and amphibians (Berger et al. 2011). To restore degraded kettle holes and develop appropriate conservation strategies, it is essential to know their pre-disturbance reference state and to understand the natural and anthropogenic factors that influenced their current condition.

Many limnological and paleolimnological studies have shown that P is the key nutrient that regulates trophic status (Håkanson 2005; Kleeberg et al. 2010). Other factors that influence lake trophic state include catchment features (e.g. slope, soil type), the hydrologic budget, and the size and form of water bodies, which can regulate transport processes such as erosion and sedimentation and internal P loading. These processes ultimately govern many trophic state variables, such as P concentration and water clarity, which regulate primary and secondary production (Wetzel 2001).

We report the results of a paleolimnological investigation that compared the recent histories of the two kettle holes using core stratigraphy to document their sediment burden, eutrophication trajectory and modern trophic state. Our goal was to evaluate their biogeochemical responses to recent environmental changes. This study addressed two specific questions pertaining to the past and modern P status, given the history of agricultural activity in the catchments: (i) How have the magnitude of sediment yield and supply of P and its binding partners changed through time? (ii) What factors currently control internal P cycling? Our approach was designed to elucidate the timing and impact of P loading on kettle holes and make it possible to disentangle natural from anthropogenic influences on kettle hole P status, primary production and associated ecological factors.

Materials and methods

Study sites and background settings

Kettle holes are a characteristic feature of Uckermark, the largest county in the federal state of Brandenburg, approximately 80 km north of Berlin in NE Germany (Fig. 1). The young moraine landscape of the same name (Uckermark) covers 3058 km^2, extending up to 71 km from north to south and 81 km from east to west. It ranges in altitude from −1.0 m below sea level in the lower Oder River Valley to 139.5 m above sea level in Blocksberg. The area has only ~40 inhabitants km^{-2}, making it one of the most sparsely populated areas in Germany. The Uckermark region is characterized primarily by agricultural areas (62.7 %, mainly cereals), forests (24.4 %) and water (5.0 %); the rest are residential areas and areas of other utilization.

Around 1800, badlands and wastelands amounted to one third of the arable land in the Uckermark. By 1864, only about 6.2 % of the area was not under cultivation (Bayerl 2006). During the agrarian reform of the eighteenth and nineteenth centuries, many measures, including land drainage, were undertaken to improve the value of soils for agriculture. Agrarian reform in the former German Democratic Republic (1948–1950) led to the industrialization of agriculture and to extreme changes in the Uckermark (Meine 2014). As a result of land consolidation and collectivization in the 1950s and 1960s, fields became larger, averaging 50 ha, but up to 200 ha, and there were almost no erosion-inhibiting structures (Bayerl 2006). As a consequence of widespread land clearance, dewatering measures (fen depletion, soil compaction) and agricultural intensification, soils became degraded and highly susceptible to water and wind erosion. Secondary alteration and decomposition processes led to a loss of organic matter (humus) from topsoils, which then exhibited a powdery-dusty to fine polyhedric grain and aggregate texture (Meine 2014).

Our study area, the young moraine landscape of NE Germany, contains approximately 150,000 to 300,000 kettle holes (potholes) that range in size from 0.01 to 3 ha (Kalettka and Rudat 2006). Most formed at the end of the last glaciation, approximately 12,000 years ago, from the slow melting of buried ice blocks (Kalettka et al. 2001). Two semi-permanent kettle holes (Table 1; Fig. 1) close to the villages of Rittgarten and Kraatz were studied and were hereafter

Fig. 1 Map showing Germany and the study area Uckermark with the kettle holes Rittgarten and Kraatz as well as their bathymetric maps
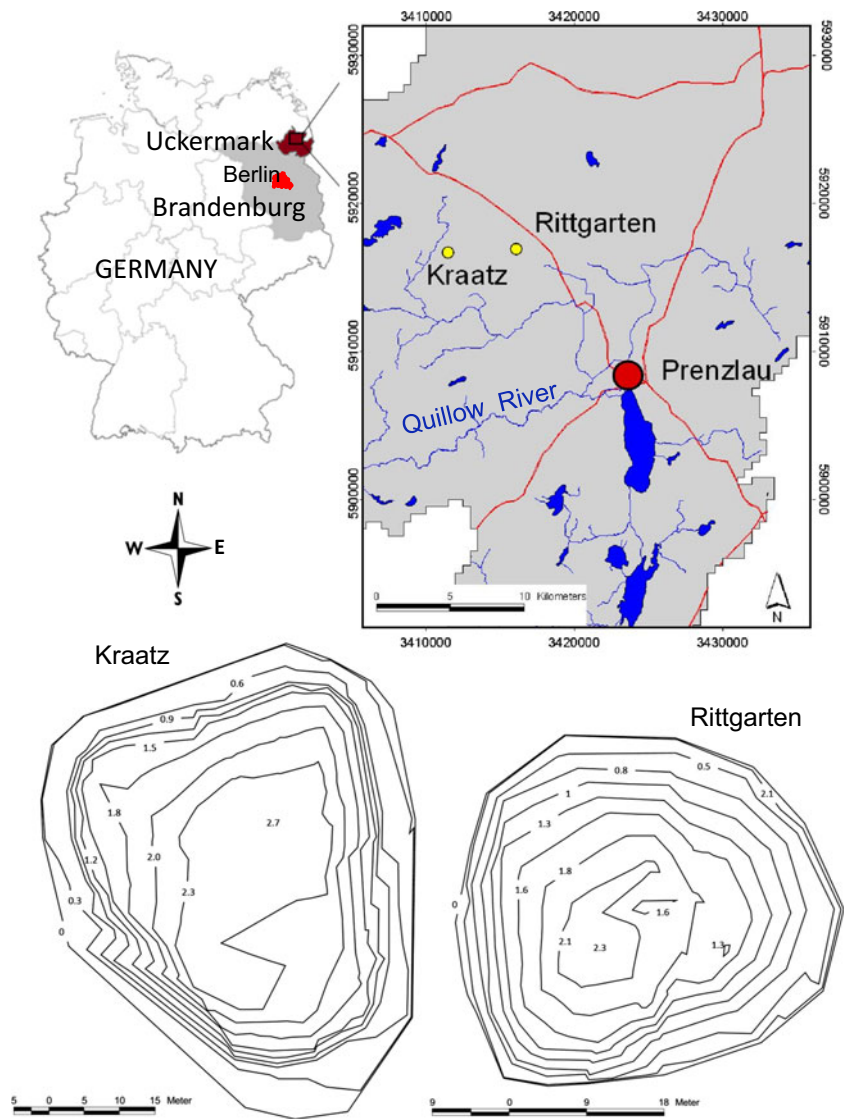
referred to as RG and KR, respectively. Sandy soils with low to medium exposure to erosion prevail in the 5.7-ha RG catchment (GeoBasis 2014). On hilltops, mixed rendzina and calcareous brown soils dominate; on the middle of hillsides, calcareous brown soils dominate, and in the lowest areas, gleyed coluvisols prevail. In the KR catchment (3.4 ha), loamy soils with a medium to high exposure to erosion prevail (GeoBasis 2014). On hilltops and along upper slopes, mixed rendzina prevails; on middle slopes, pseudo-gleyed luvisols and eroded luvisols are dominant, and on both the lower slopes and in the depression, gleyed coluvisols dominate.

Sediment core sampling and analysis

Two undisturbed sediment cores (6-cm diameter) were taken at the maximum depth in each kettle hole (Table 1) using a UWITEC© (Mondsee, Austria) corer on 19 June 2013. The RG$_1$ core was 31 cm long, and the KR$_1$ was 51 cm long. Both sediment cores were cut in half length-wise. One core half was used to determine metal concentrations at 500-μm resolution along the core by micro-X-ray fluorescence (μXRF), using an ITRAX core scanner (Cox Analytical Instruments, Mölndal, Sweden). Detailed methods are described elsewhere (Croudace et al. 2006). The other core half was sliced into 1-cm intervals that were analysed by conventional methods to convert the semi-quantitative μXRF data (counts) into concentrations [mg g^{-1} dry weight (dw)] by correlation (Neyen 2014).

Two additional sediment cores (RG$_2$ 29 cm long, KR$_2$ 54 cm long) were taken at the same sites on 10 October 2013 for dating and other analyses. These sediment cores were also sectioned at 1-cm intervals. Aliquots of sediment wet weight (fw) were used to determine the dw (105 °C, 8 h). From the dw, the proportion of organic matter (OM) was determined as loss on ignition (LOI) at 450 °C for 3 h. Organic carbon (C$_{org}$) was estimated as C$_{org}$ = OM × 0.5 (Brenner and

Table 1 Morphometric characteristics (19 June 2013) and range, mean and standard deviation of water chemistry variables from the studied kettle holes at Rittgarten (E 013°, 42′, 09″, N 53°, 23′, 22″) and Kraatz (E 013°, 39′, 48″, N 53°, 25′, 05″) between April and December 2013 ($n = 16$ occasions)

	Rittgarten	Kraatz
Volume (m^3)	1797	3998
Area (m^2)	1459	2689
Maximum depth (m)	2.34	2.64
Mean depth (m)	1.23	1.48
Conductivity ($\mu S\ cm^{-1}$)	430–568 497 ± 37	158–372 221 ± 53
pH (−)	6.9–8.5 7.2 ± 0.4	6.9–7.7 7.3 ± 0.3
Chlorophyll a ($\mu g\ L^{-1}$)	5–81 22 ± 24	2–8 4 ± 2
Suspended particulate matter ($mg\ L^{-1}$)	1.8–33.0 7.0 ± 7.8	1.0–21.5 6.6 ± 6.9
Total phosphorus ($mg\ L^{-1}$)	0.03–0.39 0.06 ± 0.04	0.03–0.16 0.09 ± 0.05
Soluble reactive phosphorus ($mg\ L^{-1}$)	0.01–0.33 0.11 ± 0.11	0.01–0.07 0.03 ± 0.02
Total nitrogen ($mg\ L^{-1}$)	1.79–3.49 2.34 ± 0.51	1.0–1.4 1.18 ± 0.11
Ammonium-N ($mg\ L^{-1}$)	0.01–0.51 0.11 ± 0.12	0.09–1.0 0.15 ± 0.26
Nitrate-N ($mg\ L^{-1}$)	0.01–0.35 0.04 ± 0.09	0.01–0.03 0.02 ± 0.01
Chloride ($mg\ L^{-1}$)	20.6–24.4 23.0 ± 1.3	9.3–12.9 10.8 ± 1.2
Sulphate ($mg\ L^{-1}$)	18.2–43.2 22.7 ± 6.5	8.7–9.8 9.0 ± 0.3

Binford 1988). Concentrations of Fe, P, Ca, Cd, Cu, K, Mn, Mo, Pb, Zn and Si were determined after wet digestion of dry, weighed samples in aqua regia ($HCl:HNO_3$ 3:1) in a microwave (1600 W, 160 °C, 20 min), followed by inductively coupled plasma optical emission spectrometry (ICP-OES) using an ICP-iCAP 6300 DUO (Thermo Fisher Scientific, GmbH). Fe and total P (TP) were also determined after wet digestion of the ash (1 N HCl, 120 °C, 20 min) produced from the OM determination (Andersen 1976). After neutralization and filtration (0.45 μm), the TP concentration was photometrically determined as soluble reactive P (SRP) by the molybdenum-blue method (Murphy and Riley 1962), and Fe was determined by the phenanthroline method (Tamura et al. 1974). Concentrations of C, N and S were determined on an elemental analyser TruSpec CNS (Leco Instruments, GmbH). All determinations were performed in duplicate. For more methodological details, see Neyen (2014). To consider the sediment heterogeneity, similar to that of the sedimentation flux (Kleeberg et al. 2015), both dw, TP and Fe of the first (RG_1, KR_1) and second set of cores (RG_2, KR_2) were cross-

correlated. The overlap and time lag, respectively, for RG_1 and RG_2 varied between 2 years for dw and 3–5 years for TP and Fe; for KR_1 and KR_2, between 3 years for dw and 4–5 years for TP and Fe.

Core dating

Cores RG_2 and KR_2 were analysed for ^{210}Pb and ^{137}Cs activity to determine age-depth relations and constant sediment accretion rates (SAR) for the past 150–200 years. Dry weight, total P and Fe were also determined as described above. Aliquots of dw were homogenized and placed in glass vials prior to gamma-spectrometric analyses. A high-purity germanium well detector with a relative efficiency of 40 % (energy range 40 keV–2 MeV) was used. Depending on the sediment mass available, measurement time varied from 1 to 6 days. Activities of natural ^{210}Pb (46.5 keV) and ^{238}U were determined. ^{226}Ra was determined via the short-lived decay radionuclides of ^{222}Rn (^{214}Pb and ^{214}Bi), and the equilibrium between ^{226}Ra, ^{222}Rn, ^{214}Pb and ^{214}Bi was evaluated according to DIN ISO 18589–3 (2014). The ^{210}Pb fraction used for dating is the unsupported (excess) ^{210}Pb ($^{210}Pb_{unsupp} = ^{210}Pb_{total} - ^{226}Ra$ (i.e. $^{210}Pb_{supported}$)) and is assumed to be supplied to the lake sediment at a constant rate from the atmosphere. The constant rate of supply (CRS) model (Appleby and Oldfield 1978), which can accommodate varying SAR, was applied. The cumulative dry matter per area (CDMA) was calculated using the weighted mean of the density of the different sediment constituents, i.e. OM, 1.5 g cm^3 and mineral solids, 2.5 g cm^3 (Binford 1990).

Anthropogenic ^{137}Cs, with a gamma energy of 661.7 keV, was measured in the same core increments analysed for ^{210}Pb to provide an independent check on the ^{210}Pb chronology. Nuclear weapon tests between 1945 and 1980 injected large amounts of artificially produced ^{137}Cs (half-life = 30.1 years) into the atmosphere. Cesium-137 deposition rates in the environment showed a pronounced maximum in 1963. Because ^{137}Cs is strongly bound to clay minerals, the 1963 weapons' testing peak is preserved in most sediments (Nehyba et al. 2011). A further time marker that was more pronounced than the 1963 peak originates from the Chernobyl reactor accident (former Ukrainian SSR of Soviet Union) in 1986.

Principal component analysis

Multivariate data sets of core element concentrations typically exhibit numerous bivariate correlations because a single process often affects more than one element. An inverse approach can help identify the important processes because each process or influencing variable imprints a characteristic pattern on the elemental concentration. Thus, principal component analysis (PCA) is often used (Donner and Witt 2006; Hermanns and Biester 2013; Villasenor et al. 2015). For a comprehensive

introduction to PCA, see Jolliffe (2002). The two analytical data sets of both kettle holes were merged by averaging the μXRF data (RG₁, KR₁) within the respective 1-cm layers. Merging data from different sites is quite common in hydrology and geochemistry (Selle et al. 2013) and results in adding information compared to performing a separate analysis for each data set, thus better disentangling the site-specific peculiarities. To achieve equal weighting of the different variables irrespective of the different ranges and variances of values, the data were normalized to zero mean and unit variance for each variable. Analysis was performed using R software (R Core Team 2014).

Results

Sediment lithology

Sediment in cores from RG₁ and KR₁ is comprised of fine detritus mud, and particles were generally uniform and fine-grained (silt- and clay-sized). The RG sediment is currently influenced by the accumulation of the common reed *Phragmites australis* (Cav.) Trin ex. Steud., the soft hornwort *Ceratophyllum submersum* L., and the common duckweed *Spirodela polyrhiza* (L.) Schleid. In contrast, the KR₁ core had a few bits of discrete macrophyte debris in the upper sediment horizons, which originated mainly from shoreline vegetation and the broad-leaved pondweed *Potamogeton natans* L.

Core chronology and sediment accretion rate

Unsupported ^{210}Pb activity in both cores (RG₂, KR₂) generally displayed a down-core monotonic decline but showed some intervals in which activity was unchanged or even increased with greater depth, reflecting changes in SAR. An additional time marker is the ^{137}Cs peak from the Chernobyl reactor accident in 1986, which is recorded in much of Europe, including our study site Uckermark (Fig. 1).

In RG₂, CDMA increased relatively constantly from 0.5 kg m^{-2} in the uppermost centimetre to 177.7 kg m^{-2} at 28 cm depth (Fig. 2). Unsupported ^{210}Pb decreased fairly monotonically down-core. Specific activity of ^{137}Cs increased from 49 Bq kg^{-1} in the uppermost sediment layer to a maximum of 101 Bq kg^{-1} at 5.5 cm depth, representing the year 1986. The second maximum of 88 Bq kg^{-1}, at 10.5 cm depth, identifies the year 1963 (Fig. 2). In KR₂, unsupported ^{210}Pb decreased from 139 Bq kg^{-1} in the uppermost layer to much lower values between 5.5 and 11.5 cm depth but increased again to higher values between 14.5 cm (86 Bq kg^{-1}) and 26.5 cm depth (74 Bq kg^{-1}). Below that depth, ^{210}Pb$_{unsupp}$ decreased with depth to 0 Bq kg^{-1} at 53.3 cm. Distinct ^{137}Cs peaks occur at 15.5 cm (116 Bq kg^{-1}) and 27.5 cm

(89.5 Bq kg^{-1}), representing the years 1986 and 1963, respectively (Fig. 2).

In RG₂, the SAR averaged 2.1 ± 0.2 mm year^{-1}, the upper 1 cm layer belonged to 2013 ± 0.2 years and the 20.5 cm horizon extended back to 1910 ± 6 years (Fig. 3). Extrapolated ages, assuming a constant sediment accumulation rate, suggest the base of the core dates to ca. 1857 ± 9 years. The SAR increased from 2.0 mm year^{-1} in 1910 to 2.9 mm year^{-1} in 2013, the corresponding sediment accumulation increased from 0.07 g cm^{-2} year^{-1} to 0.25 g cm^{-2} year^{-1} (Fig. 3). In KR₂, the mean SAR was 4.9 ± 0.8 mm year^{-1}, the upper 1 cm layer belonged to 2013 ± 0.5 years and the core extended back to 1907 ± 8 years. SAR increased from 0.2 mm year^{-1} around 1900 to 6.3 mm year^{-1} in 2013 and varied considerably since the early 1980s (Fig. 3). The sediment accumulation rate increased from 0.2 ± 0.008 g cm^{-2} year^{-1} around 1900 to 0.66 ± 0.21 g cm^{-2} year^{-1} in recent years (2009–2013).

Chronology of organic matter, carbon, nitrogen and phosphorus accumulation

In RG₁, dw decreased rather consistently towards the sediment surface (Fig. 4). The proportion of OM was relatively constant in deeper layers (15–30 cm), peaked at 13 cm depth and increased continuously from 17.8 % at 10 cm depth to 65.8 % at the sediment surface. Concentrations of total N and S tracked OM content closely, reaching maxima of 26.8 and 24.1 mg g^{-1} in surface deposits, respectively. The C$_{org}$/N ratio (which can be deduced from Fig. 4) changed little over the core, from 13.9 at the maximum depth to 11.3 at the sediment surface.

In KR₁, dw showed considerable stratigraphic variation, with small peaks at 44 cm (~1920) and 24 cm (~1963) depth and an 8-cm-thick layer of a higher dw from 4 to 12 cm depth (Fig. 4). This layer had a relatively constant (7.3 ± 0.5 %, $n = 9$) and lower OM proportion than deeper deposits (20.3 ± 1.3 %, $n = 9$) or the overlying sediment layer (21.9 %). Overall, the OM proportion in KR₁ was much lower than that of RG₁. The maxima of N (9.8 mg g^{-1}) and S (18.2 mg g^{-1}) for KR₁ were at 13.5 cm depth. The C$_{org}$/N ratio (which can be deduced from Fig. 4) was relatively constant over the core length, from 18.2 at the maximum depth in the core to 17.3 at the sediment surface, but was higher than in RG₁.

In RG₁, sediment TP increased up-core, peaked at 14.5 cm depth, coinciding with the peak in OM (Fig. 4), and decreased to a near-constant value of approximately 1 mg g^{-1} (Fig. 5). The K concentration exhibited a low at 13 cm depth (~1924) and peaked at approximately 10 cm depth (~1943). The Ca concentration decreased slightly up-core, from 7.4 ± 0.8 mg g^{-1} (n = upper 20 cm) at the bottom to 6.0 ± 0.3 mg g^{-1} (n = lower 20 cm) at the top of the core. The Si concentration oscillated, with two distinct minima, at 13 cm

Fig. 2 Vertical distribution of cumulative dry matter per area (CDMA, kg m^{-2}), and ^{137}Cs, and unsupported ^{210}Pb activities (Bq kg^{-1}) in sediment cores from the Rittgarten (RG$_2$) and Kraatz (KR$_2$) kettle holes. *Arrows* indicate peaks in ^{137}Cs activity, reflecting known emission events in 1963 (fallout maximum from atmospheric bomb testing) and 1986 (nuclear accident at Chernobyl)
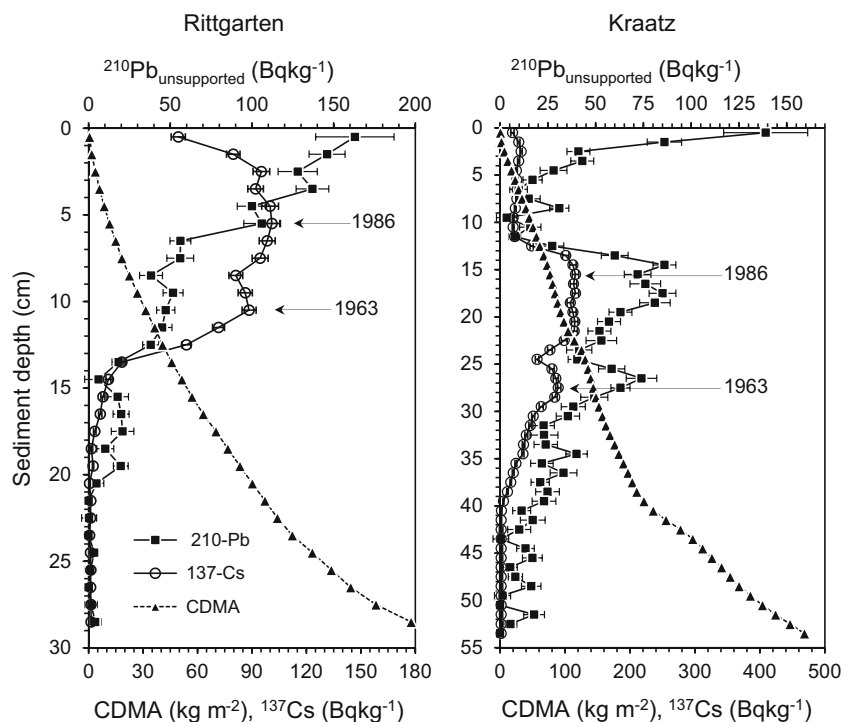
depth (1.0 mg g^{-1}) and at the sediment surface (1.1 mg g^{-1}), and a maximum at 10 cm depth (2.4 mg g^{-1}).

In KR$_1$, sediment TP increased slightly up-core and reached a maximum of 2.0 mg g^{-1} at the sediment surface (Fig. 5), about twofold higher than surface TP in RG$_1$. In the layer between about 11 and 1 cm depth, which consisted of

OM-poor deposits (Fig. 4), the concentration of K was only slightly enhanced (6.9 ± 0.4 mg g^{-1}, $n = 220$) compared to the layers down to the bottom (6.3 ± 0.5 mg g^{-1}, $n = 800$), whereas Ca values were elevated (7.8 ± 1.2 mg g^{-1}) compared to values 4.6 ± 0.6 mg g^{-1} deeper in the core. Silicon concentration increased at a depth of 11 cm if compared to the layers directly

Fig. 3 Sediment accretion rate (SAR) and sediment accumulation rate according to the constant rate of supply model (unsupported ^{210}Pb, Fig. 1), as corrected by the ^{137}Cs peaks (Fig. 2), for the Rittgarten (RG$_2$) and Kraatz (KR$_2$) kettle holes
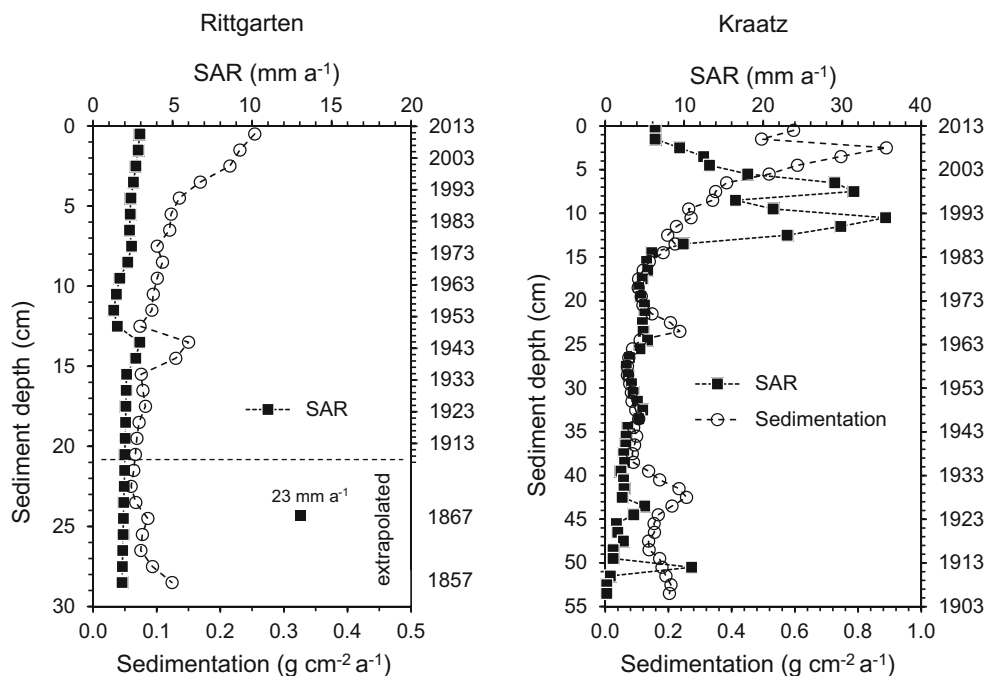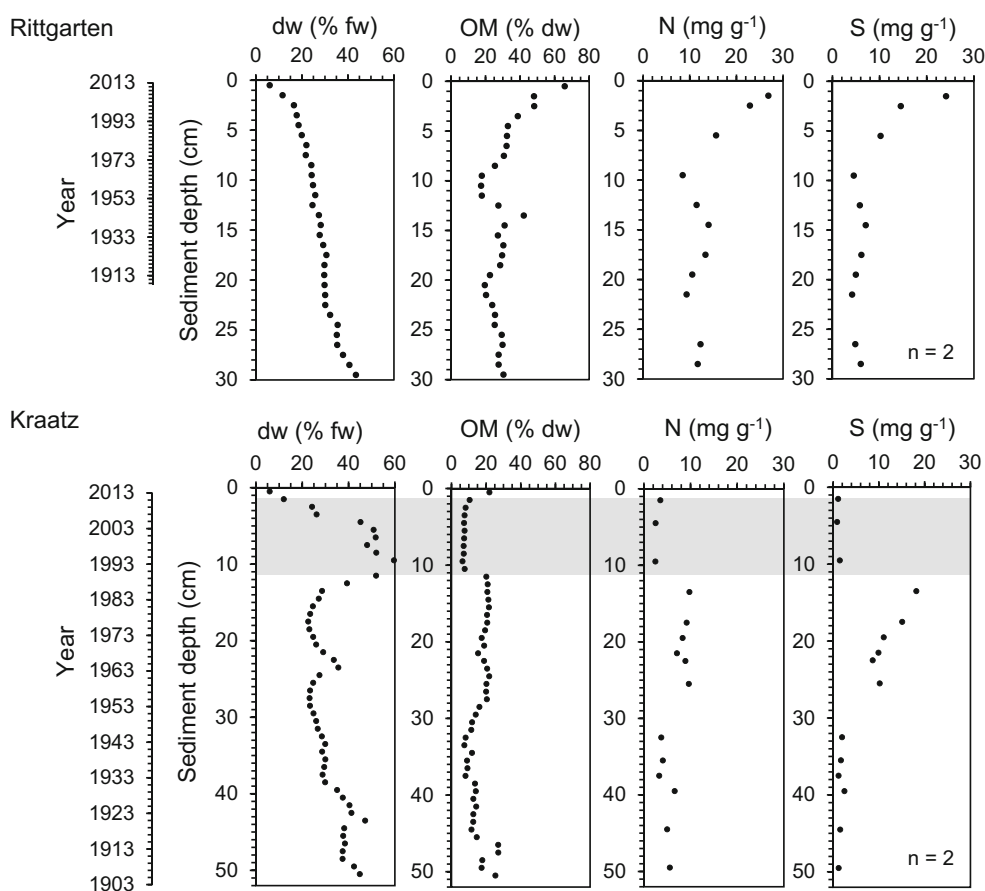
Fig. 4 Sediment percent dry weight (*dw*), and organic matter (*OM*), total nitrogen (*N*) and total sulphur (*S*) per g dw versus depth and date in the Rittgarten (*RG₁*) and Kraatz (*KR₁*) sediment cores. The *grey area* depicts two massive erosion periods (see Fig. 3)

below, but the mean of the upper 11 cm layer (1.1 ± 0.01 mg g^{-1}, $n=220$) did not differ from all the deeper layers of the core (1.1 ± 0.01 mg g^{-1}, $n=800$).

Chronology of metal accumulation

In RG₁, the sediment Fe concentration oscillated, with maxima of ~38 mg g^{-1} at about 1913, 1945, and at the sediment surface (2013) (Fig. 6). Fe net accumulation increased from 2.3 g m^{-2} year^{-1} ca. 1910 to 7.34 g m^{-2} year^{-1} in 2013. The Mn concentration also exhibited a generally decreasing trend up-core. Zinc concentration was relatively constant over the length of the core (98.2 ± 10.3 µg g^{-1}, $n=622$) except for a few high values at 17 cm depth, suspected of being outliers. The Cu concentration remained relatively unchanged between 30 and 13 cm depth (44 ± 9 µg g^{-1}; $n=161$) but was higher between 13 and 8 cm depth (68 ± 12 µg g^{-1}; $n=101$) and lower and relatively constant in the upper 8 cm (36 ± 7 µg g^{-1}; $n=362$).

In KR₁, Fe concentration was similar to values in RG but did not vary as much, displaying only a slight increasing trend up-core. The Fe net accumulation rate increased from 1.74 g m^{-2} year^{-1} around 1900 to 7.82 g m^{-2} year^{-1} in 2013. Mn also shows a slight up-core increase in

concentration but displays elevated values at 49, 40 and 37 cm depth (i.e. ~1909, 1928 and 1935). Two further peaks appeared at 10 and 2 cm depth, i.e. at the lower and upper margins of the OM-poor layer (Fig. 4). The Zn concentration over the whole core averaged 224 ± 21 µg g^{-1} ($n=1022$) and was thus twofold higher than in RG₁. Between 50 and 27 cm depth (~1907–1955), Zn concentration oscillated between 190 and 301 µg g^{-1}. Between 27 and 11 cm (~1955–1989), Zn concentration was constant at 200 ± 7 µg g^{-1} ($n=321$), whereas between 11 and 2 cm depth, the Zn concentration increased from 193 to 259 µg g^{-1}, in concordance with the increase in Fe concentration (Fig. 6). The Cu concentration in KR₁ was virtually constant (21.2 ± 2.4 µg g^{-1}; $n=1022$) over the whole depth profile.

Molar Fe/P ratios between 1909 and 2013 showed no clear trend and were similar between RG₁ (18.5 ± 9.0, $n=19$) and KR₁ (18.4 ± 5.2, $n=51$). The molar S/Fe ratio in RG₁ increased from 0.4 around 1857 to 2.3 in 2013, whereas in KR₁, this ratio did not show any distinct trend (0.3 ± 0.4) over the whole core (not shown).

In RG₁, Mo concentration was slightly elevated at 1.9 ± 0.3 µg g^{-1} ($n=322$) between 30 and 15 cm depth and decreased further, while oscillating up-core to 3.2 µg g^{-1} at the sediment surface (Fig. 7). Stable Pb and Cd concentrations

Fig. 5 Sediment total phosphorus (*P*), potassium (*K*), calcium (*Ca*) and silicon (*Si*) concentrations per gramme dw versus depth and date in cores from the Rittgarten (*RG₁*) and Kraatz (*KR₁*) kettle holes
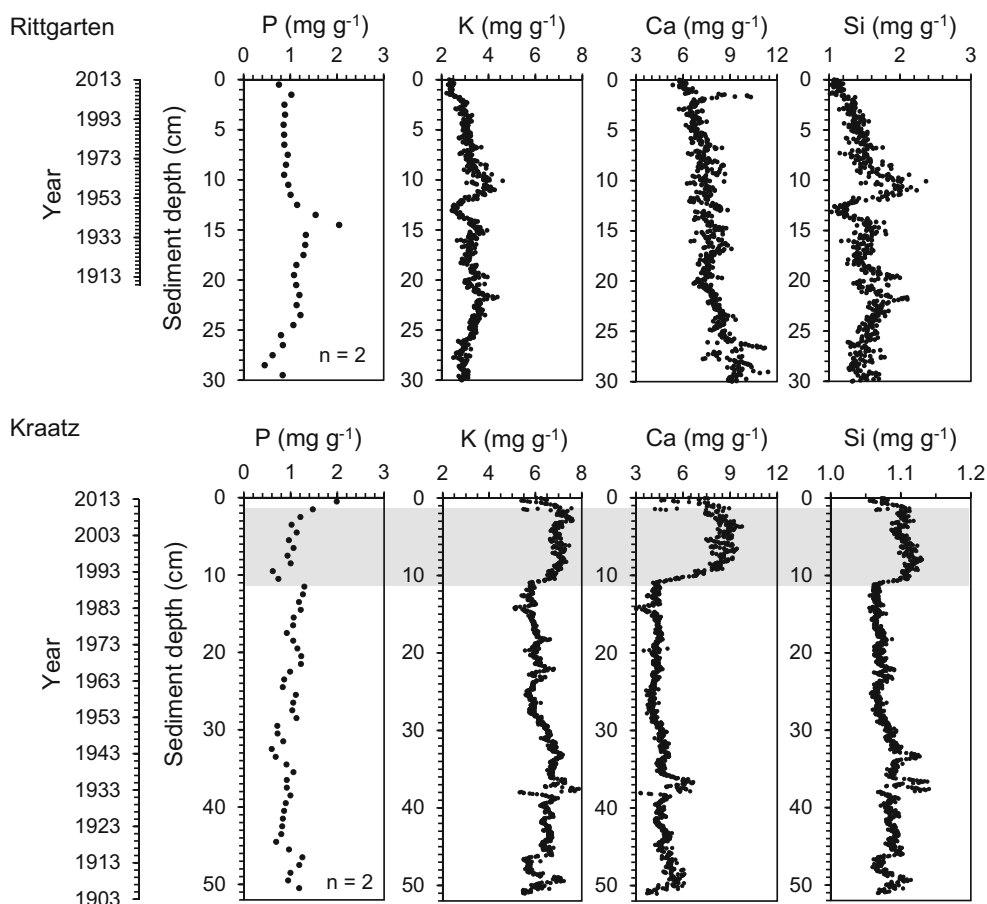
were constant over the whole core in a scattered distribution around a 'baseline' of approximately 30 and 0.8 μg g^{-1}, respectively. Zr counts decreased slightly up-core, i.e. from 2.46 ± 0.33 × 10^3 cps at 29–30 cm depth ($n = 10$) to 1.85 ± 0.18 × 10^3 cps at 0–1 cm (Fig. 7).

In KR$_1$, the constant Mo concentration over the whole profile (1.1 ± 0.07 μg g^{-1}, $n = 1025$) can be regarded as background, if compared to RG$_1$ (Fig. 7). The Pb concentration was of the same order of magnitude as in RG$_1$. For Cd, the baseline (detection limit) at 0.8 μg g^{-1} was similar to that in RG$_1$, but the scatter was somewhat greater. There is a general decrease in Zr concentration from 3.83 ± 0.71 × 10^3 cps at 49–50 cm depth ($n = 10$) up-core to 2.9 ± 0.71 × 10^3 cps at 9–10 cm depth, followed by a sharp increase to 5.99 ± 0.62 × 10^3 cps at 10–11 cm depth and a decrease back to 2.93 ± 0.56 × 10^3 cps at the sediment surface (0–1 cm, Fig. 7).

Results of the principal component analysis

Data from both sites were used in the PCA (Fig. 8), assuming that identical geochemical processes prevailed at both kettle holes, although possibly not to the same extent. Three principal components (PCs) with eigenvalues >1 were identified.

They covered 78 % (55, 12 and 11 % for the first, second and third PC, respectively) of the variance.

For the first PC, high positive scores are indicative of high Cd, Zr, Zn and K concentrations and, to a lesser degree, high Pb and Mn concentrations. The opposite is true for Cu, Si, Mo and C$_{org}$ (Fig. 8). Out of the first three PCs, only the first clearly differentiates between the two sites without any overlap (Fig. 8d). This PC could reflect different mineralogical composition and use of the soils at the two sites. At RG$_1$, there appears to be a systematic shift towards more negative scores, with a stepwise decrease in the late 1940s. Correspondingly, the scores of the first PC at KR$_1$ exhibited a stepwise decrease around 1970 and an increase again in the late 1990s (Fig. 8d).

The second PC is characterized by a highly positive correlation with Ca and highly negative correlation with Pb, C$_{org}$, P and water content (Fig. 8b). In addition, Zr, Si, Fe and Mn exhibit positive correlation. High positive scores thus indicate rather high mineral content, especially Ca and presumably carbonates, whereas negative scores can be ascribed to a larger water content and a larger organic fraction, including organic P. The scores of that principal component cover approximately the same range at both sites. In general, both profiles exhibit a similar remarkably long-term decrease of the scores, pointing to a long-term increase of the organic content (Fig. 8e).

Fig. 6 Sediment total iron (*Fe*), manganese (*Mn*), zinc (*Zn*) and copper (*Cu*) concentrations per gramme dw versus depth and date in cores from the Rittgarten (*RG₁*) and Kraatz (*KR₁*) kettle holes
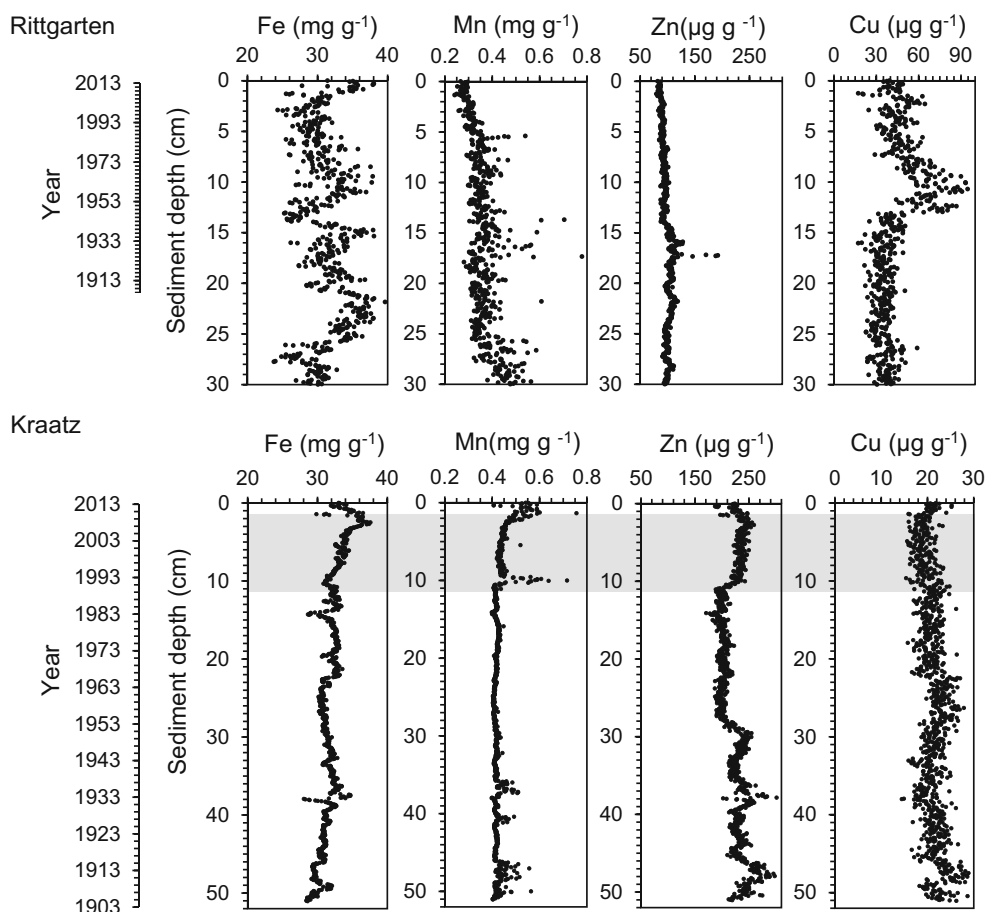
However, a major deviation form that general trend is observed for the last years at KR₁, whereas at RG₁ a major increase is observed between 1940 and 1975 and a clear decrease thereafter (Fig. 8e).

The third PC exhibits positive correlations especially with Fe and P (Fig. 8c). The depth profiles of the scores of that component run parallel to each other until 1940 and then tend to run counter to each other thereafter (Fig. 8f). In addition, exceptionally low values are observed at KR₁ during the last years.

Discussion

### Kettle holes have not been intensively studied

Except for some infrequent water quality measurements since 1992 (Lischeid and Kalettka 2012), there were no limnological data gathered from the kettle holes prior to the clear changes noted above (Figs. 4, 5, 6, and 7) and certainly none that can be used to define reference conditions (Kalettka and Rudat 2006). The use of loading estimates from other kettle holes (Frielinghaus and Vahrson 1998) to establish a general reference state for these basins is problematic because most kettle

holes have been manipulated or impacted to some degree (Kalettka et al. 2001; Berger et al. 2011; Altenfelder et al. 2014). Thus, paleolimnological methods offer the only feasible way to establish pre-disturbance conditions in kettle holes. Moreover, although many studies have pointed out the various controlling factors of sediment and nutrient delivery on a plot or watershed scale, little is known about the spatial variability of sediment and nutrient delivery on a regional scale (Verstraeten and Poesen 2002).

Even kettle holes close to each other are very different

Although only 3 km apart, the two kettles display great differences in net sediment accumulation (Fig. 2). At RG₂, the SAR profile showed a high of 2.3 cm year⁻¹ in 1867 ± 9 years and another less pronounced peak between 1940 and 1943 (Fig. 3). The first is attributed to human activities during the so-called *Flurneuordnung*, i.e. rural farmland planning (Bayerl 2006; Neyen 2014), when, for example, there were attempts to fill the hollow to gain more farmland. Between 1940 and 1943, higher SAR reflects intensification of agriculture during World War II, a consequence of *Reichsnährstandsgesetz*, i.e. the Law of Nutritional Level of the German Reich (Neyen 2014). Elevated SARs (Fig. 3) are

Fig. 7 Vertical distribution of sedimentary total molybdenum (*Mo*), lead (*Pb*), cadmium (*Cd*) and zirconium (*Zr*) on a dw basis in the Rittgarten (*RG₁*) and Kraatz (*KR₁*) kettle holes
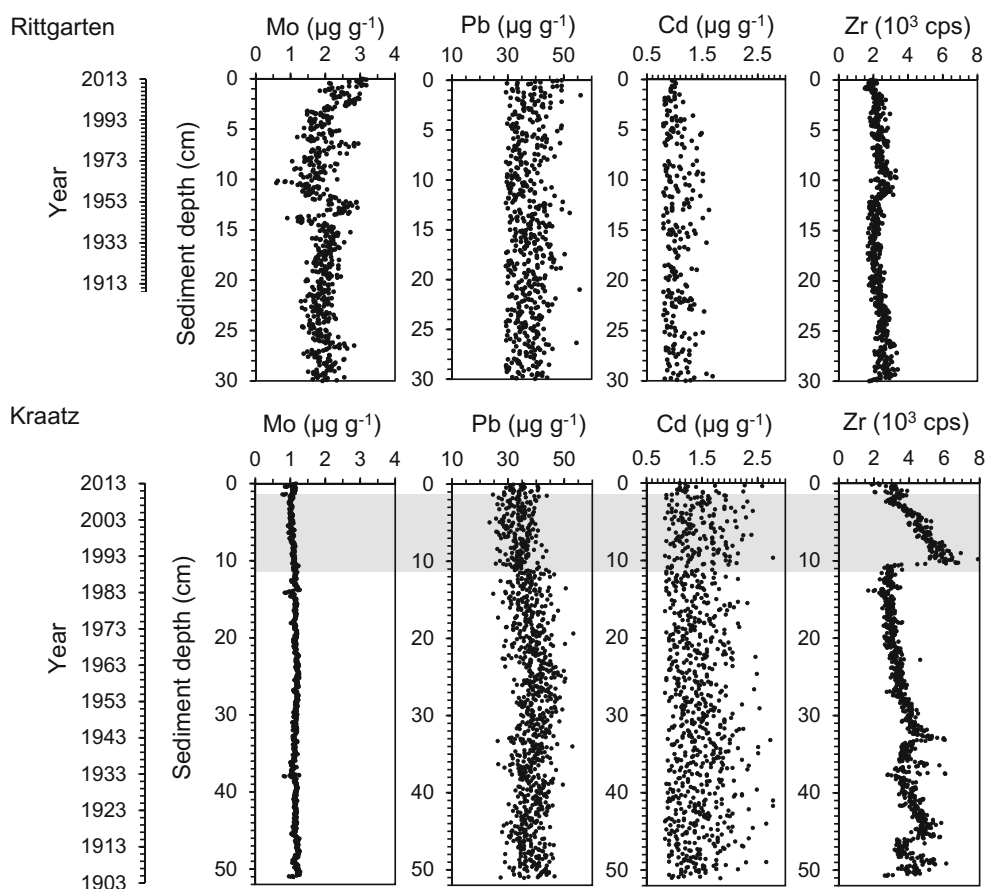
attributed to greater erosion events, although the input of aeolian sediments and their constituents (metals, nutrients) during storm events cannot be ruled out. The kettle hole at RG has a very small catchment and only rainfall maintains the water level, so the relatively low SAR compared to other kettle holes (Gąsiorowski 2008; Begy et al. 2009) appears to be realistic and is similar to those determined for kettle holes surrounded by cropland (Preston et al. 2013). In RG$_2$, SAR showed an overall increasing trend since 1894 ± 7 years. Reasons for this might be the positive trend in winter precipitation, leading to erosion in the absence of vegetation and increasing intensification of land use (Battarbee et al. 2005; Rose et al. 2011). In addition, as is known for other lake types, the strong effects of climate change on summer surface water temperature (Vincent 2009) may contribute to an intensification of the turnover of matter and nutrients in the very shallow kettle holes.

In KR$_2$, the SAR profile is highly variable (Fig. 3) probably because the catchment at KR has steeper slopes and therefore experiences greater erosion than RG$_2$ (Neyen 2014). As at RG, the main impacts at KR were anthropogenic. However, in the absence of historic sources, the direct influence of ploughing or heavy rain, for example, on erosion remains uncertain. Nevertheless, as stated for

RG, there was an intensification of agriculture during World War II. Moreover, starting in 1983, there was the next massive increase in the SAR also caused by intensification of agriculture in the area (Bayerl 2006). This period of enhanced sediment accumulation over approximately 30 years cannot solely be attributed to a single erosion event. Rather, it is the result of sustained transport of soil constituents to the KR kettle hole. Our SAR values are similar to the mean constant accumulation rate determined for a kettle hole 50 km east of Berlin, Lebuser Platte, which was approximately 0.1 to 0.2 cm year^{-1} from the fourteenth century to 1960 and increased to 0.5 cm year^{-1} after 1960 because of intensified cultivation (Frielinghaus and Vahrson 1998). Preston et al. (2013) reported that the constant SAR from wetlands surrounded by croplands was 2.7 and 6 times greater than in wetlands surrounded by native prairie.

In RG$_1$, the steady dw decline through time coincides with an increase in OM and its constituents (Fig. 4). In general, an increase in OM in kettle hole sediments indicates increasing in-pond productivity; low OM is indicative of erosive conditions in the watershed. In KR$_1$, higher erosion is reflected in a layer with higher dw and lower OM, including N and S, compared to RG (Fig. 4).
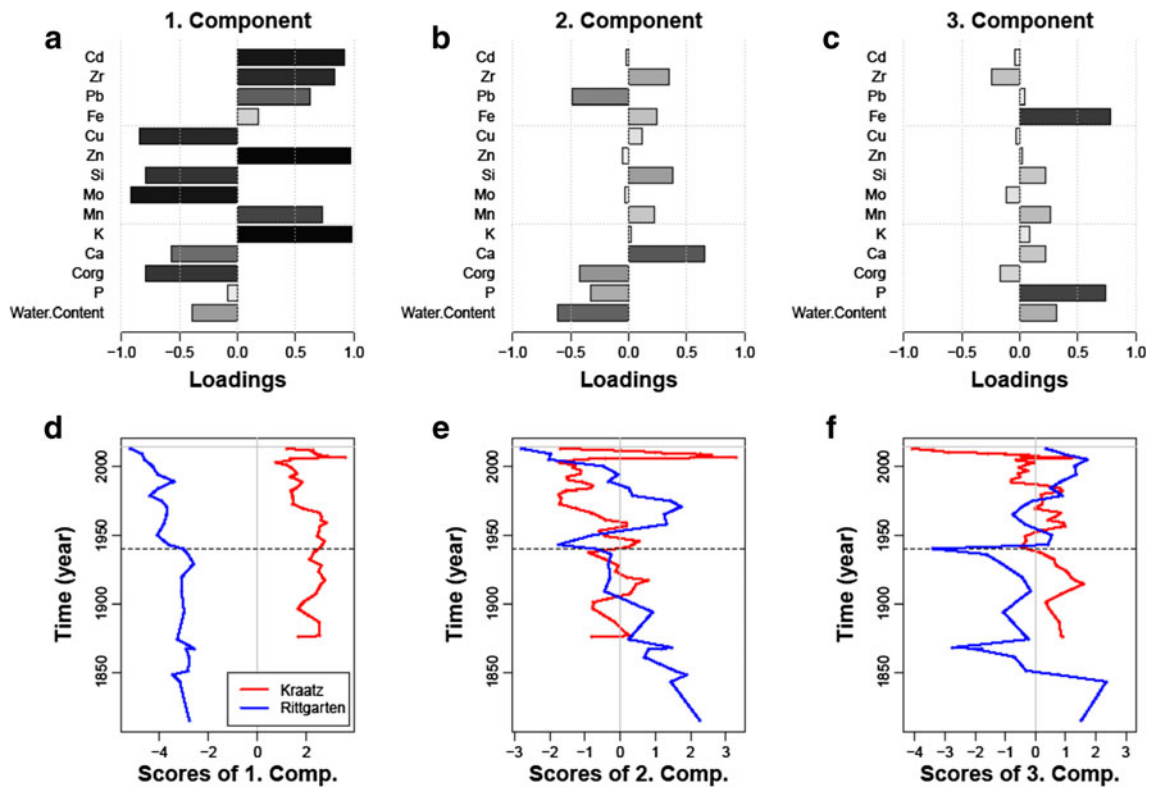
Fig. 8 Results of principal component analysis. Loadings on the first three principal components (**a**–**c**) and profiles of the scores of the first three components for kettle holes Rittgarten and Kraatz (**d**–**f**)

Iron input determines the phosphorus retention and mobility

At steady state, P input to kettle holes should equal P retention in the sediment. With an increasing SAR at RG_2 from 0.4 mm year^{-1} around 1860 to 2.8 mm year^{-1} in 2013 (Fig. 3), annual P input increased from 0.65 to 1.67 kg ha^{-1}. In KR_2, the SAR increased from 0.2 mm year^{-1} around 1900 to 6.3 mm year^{-1} in 2013 (Fig. 3), and the annual P input increased from 0.6 to 4.1 kg ha^{-1}. For comparison, a source apportionment of P emissions in the Oder River basin (area 118,148 km^2, 134 inhabitants km^{-2}), representing a substantial part of the Uckermark, showed that a relatively large proportion of the average annual P emissions to surface waters originated from agriculture; the total P export from the river basin was 0.38 kg ha^{-1}; the total P input to surface waters was 1.09 kg ha^{-1}; and the total P loss from agriculture was 0.19 kg ha^{-1} (Kronvang et al. 2005). These figures are rather low compared to total P export of between 1.8 and 39.7 kg ha^{-1}, deduced from the input into small retention ponds in central Belgium (Verstraeten and Poesen 2002).

In both kettle holes, along with an increasing SAR (Fig. 3), Fe input and retention increased (Fig. 6), reflecting the basic geology of the catchment. Concurrently, the sedimentary P concentration also increased (Fig. 5). As a result, the molar Fe/P ratio, an indicator of P mobility, remained more or less

constant over the last 100 years and was the same in both kettle holes. Thus, higher TP concentration in the water of RG compared to KR (Table 1) is either the result of a higher P input or lower Fe availability in the sediment. At a molar S/Fe ratio <1.5, vivianite, an iron phosphate mineral ($Fe_3(PO_4)_2 \cdot 8H_2O$), can be formed (Rothe et al. 2015). In RG, this threshold is currently exceeded, whereas in KR it is not, indicating that less Fe is available for P binding in RG_1 compared to KR_1. RG was densely covered by common duckweed *S. polyrhiza* (L.) Schleid, promoting oxygen depletion and effective sulphate reduction (Kleeberg et al. 2015); alternatively, KR was characterized by a modest coverage of the broad-leaved pondweed *P. natans* L. and other submersed hydrophytes.

Metal distribution indicates continuous and pulsed losses in the catchment

In Figs. 5, 6, and 7, single points in the μXRF results were not removed (as outliers) to illustrate the fine resolution and scatter of the method and the possibility to record event-related high inputs. Each dot represents 500-μm resolution, i.e. a thinner sediment layer than for SAR (Fig. 3). The profiles of K, Ca and Si (Fig. 5) reveal a different degree of mobilization from catchment soil and accumulation in the sediment. These elements in the sediment are generated by soil erosion at KR,

as visible in their temporal increase (grey area in Fig. 5). However, if there are not enough binding sites for K, as in the light soils of RG, it will be translocated to deeper soil layers (Guhl and Marquardt 2009) and possibly further via ground water to the kettle hole. At RG, most depth profiles of the sandy soils were almost completely decalcified (C. Hoffmann, Leibniz Centre for Agricultural Landscape Research, pers. comm.). Finally, elements accumulated in the kettle holes represent the sum of materials delivered directly by atmospheric deposition, those held up temporarily in surface soils and delivered by occasional erosion and elements transported by inflowing surface and ground water (Karasiewicz et al. 2014; Gołdyn et al. 2015).

Past and recent sediments are uncontaminated to moderately contaminated by heavy metals

Heavy metal concentrations in sediments (Figs. 6 and 7) are compared to those of various guidelines (Table 2) to evaluate changes in accumulation from the past (background) to recent years, as well as the toxicological level (sediment quality criteria, SQC). Except for Zn in the upper sediment layers of KR_1, all sediment metal concentrations can be classified as uncontaminated to moderately contaminated according to the SQC (Ulrich et al. 2000). The high Zn concentrations correspond to sediment layers accumulated during a period of intensive erosion. Heavy metals are adsorbed very efficiently on fine soil particles, mainly on clay particles and OM, so their input can be attributed to erosion. In particular, soils intensively treated with mineral fertilizers can contain substantial amounts of heavy metals (Mortvedt and Beaton 1995; Gołdyn et al. 2015). Evaluation of the

heavy metal concentrations relative to their geochemical background and a classification of sediments in the neighbouring country, Poland (Polish Geological Institute, State Inspection of Environmental Protection), give similar results. The contents of Zn, Cu, Pb and Cd of RG_1 and KR_1 (Figs. 6 and 7) are above their Polish background equivalents (Zn 48, Cu 6, Pb 10 and Cd 0.5 µg g^{-1}), but according to the four-class sediment classification: I–unpolluted, II–moderately polluted, III–sediments of medium pollution, IV–heavily polluted (Gołdyn et al. 2015), RG_1 and KR_1 are in the range between classes I and II.

Because of the twofold conductivity of the water in RG compared to KR (Table 1), a higher burden of heavy metals was expected. This is because the conductivity of water bodies in an agricultural landscape is usually correlated with the intensity of mineral fertilization in the catchment area (Kamiński et al. 2011) and the intensity of fertilization is also related to the amount of heavy metals introduced into the fields with the fertilizers (Mortvedt and Beaton 1995). Thus, the conductivity of water and the concentration of heavy metals in the sediments of kettle holes near Poznań, Western Poland, were correlated (Gołdyn et al. 2015). Because this relationship was not significant for RG and KR, it is reasonable to assume that within a moderate range of fertilizer application, local geomorphology (Kalettka and Rudat 2006) and erosion are the key factors in metal loading scenarios. Also, Verstraeten and Poesen (2002) reported that the observed spatial variability in nutrient losses is primarily attributed to regional variations in erosion and sediment yield values and, to a far lesser degree, spatial variations in fertilizer application.

Table 2 Regional (federal state Brandenburg, NE Germany) background values of heavy metals, their thresholds according to the spoil guideline (BB RL-EvB 2001) and related sediment quality criteria (SQC) according to Ulrich et al. (2000)

Element	Background µg g^{-1}	Spoil guideline µg g^{-1}	SQC for kettle hole and depth			
			RG_1	Depth (cm)	KR_1	Depth (cm)
Zn	43[a], 34[b]	105	1	0–30	3	2–11
					1	11–27
					2	27–50
Cu	14[a], 12[b]	28	1	0–8	1	0–50
			2	8–13		
			1	13–30		
Pb	15[a], 14[b]	49	1	0–30	1	0–50
Cd	0.048[a], 0.051[b]	0.7	1	0–30	1	0–50

The SQC are as follows: *0* uncontaminated, *1* uncontaminated to moderately contaminated, *2* moderately contaminated, *3* moderately contaminated to heavily loaded, *4* heavily loaded, *5* heavily loaded to excessively loaded, *6* excessively loaded (Ulrich et al. 2000)

RG Rittgarten, core 1, *KR* Kraatz, core 1

[a] B-horizon

[b] C-horizon

Identical geochemical processes occur in the two basins but to different extents

The PCA aimed to identify the major controls on elemental accumulation in sediments by comparing the intensities of processes between the RG and KR basins (Fig. 8). Approximately half of the total variance (PC 1) was caused by systemic differences between the two sites, which can be traced back to the different compositions of the soil substrate. Zirconium, Zn and Cd, which have high loads high on this first component, are indicative of intrusive rocks such as granite, which is abundant as glacial blocks in the Uckermark. Except for Zn in KR, where the upper (2–11 cm) sediment horizon is moderately to heavily contaminated (Table 2), the sediments have no or only moderate amounts of heavy metals. This suggests that the influence of the agricultural practices involving P fertilization (Cd, Pb), manure (Cu, Zn) and pesticides (Cu) (Berger et al. 2011) is low. Nevertheless, more kettle holes need to be studied. Gołdyn et al. (2015) reported the concentrations of heavy metals (Cd, Cr, Cu, Ni, Pb, Zn) in bottom sediments of 30 small kettle holes in the agricultural landscape of western Poland. The most important factors influencing the heavy metal concentrations were maximum depth, area of the pond, its hydroperiod and pH and conductivity of the water. Low quantities of heavy metals were recorded in the sediments of small deep pond types but were high in the larger but shallower overflow types (Kalettka and Rudat 2006). In general, shallow ponds with a large surface area and larger or steeper catchments (such as KR) are more vulnerable to heavy metal contamination (Gołdyn et al. 2015).

High loadings of K could indicate granite feldspars as an important source. All of these elements are much more abundant at KR_1 compared to RG_1, as reflected in the sediments (Figs. 6 and 7). At KR, the slopes are much steeper, which could have favoured the transport of course-grained remnants of granite weathering into the depression of this kettle hole.

There was a minor shift at both sites in the last few decades pointing to a change in the source of the deposited soil material. However, given the pronounced small-scale heterogeneity of the soils in this region (Koszinski et al. 2013), this could have been caused by minor changes in erosion pathways, for instance, modified demarcation and intensified tillage after 1945 or the establishment of a bushy buffer strip at KR.

The second component obviously reflects in the first place different portions of the mineral versus the organic portion of the sediment. Not only do the sediment cores at both sites exhibit about the same range of scores but also the long-term decrease is similar at both sites, indicating a long-term increase of the organic portion at the expense of the mineral part. Part of that trend could be an increasing degree of decomposition of the organic material and increasing compaction with depth. However, this could not explain the clear deviation from the general trend at RG between 1940 and 1975 and after 2000 at KR. On the other hand, high loadings of Pb on this component could indicate an increasing input of Pb via mineral fertilizers, especially by superphosphate. Thus, it cannot be excluded that part of the observed long-term trend might be ascribed to increasing biomass growth in and close to the kettle hole due to better supply with nutrients.

High scores of the third principal component were associated with high P and Fe contents and to a lesser degree with high Mn, Si and Ca contents (Fig. 8c). This might indicate enhanced precipitation of Fe and Mn oxides and hydroxides during oxic phases and phosphate sorption to these sesquioxides. Small silicate and carbonate particles might be included during that precipitation. Parallel courses of the scores at both sites until 1940 suggest similar hydrological boundary conditions at both sites. That synchronicity breaks down after 1940 (Fig. 8f). It can only be speculated that tile drainage or other attempts to drain the kettle holes and their surroundings might have played a role. However, except for the last years at KR, the range of the scores is rather narrow after 1940 compared to the range spanned by the scores at RG prior 1940 (Fig. 8f).

Sediment cores from the two sites (Figs. 4, 5, 6, and 7) clearly differed with respect to their first component scores but were similar with regard to the second and third components. This confirms our assumption that prevailing processes are similar at the two sites. However, it does not necessarily imply that the temporal dynamics would have been the same (e.g. SAR, Fig. 3), as shown for the second and third principal components, which probably reflects differing local conditions (Lischeid and Kalettka 2012). Only large-scale events are likely to appear as synchronous in sediment cores from different sites (Donner and Witt 2006).

Intensification of agriculture intensifies processes in the kettle holes

RG and KR experienced phases of moderate and heavy agricultural intensification over long periods of time (Fig. 9), as documented by increased SARs (Fig. 3) and accumulation rates of multiple elements (Figs. 4, 5, 6, and 7). A similar trend was reported for an inland catchment area of the ground moraine landscape, Lebuser Platte, NE Germany (Vahrson and Frielinghaus 1998). At least until the fourteenth century, there were no cultivation in this landscape and almost no erosion and sediment accumulation in the kettle holes. From the fourteenth century to around 1955 (about 600 years), the SAR averaged 0.9 mm year^{-1}. From 1955 to 1995, the SAR increased to 12.5 mm year^{-1}. Our results on sediment accumulation are in concordance with those of Vahrson and Frielinghaus (1998). However, the sediment chronologies for RG_1 and KR_1 reveal that both kettle holes experienced an enhanced burden and eutrophication linked to land use changes in
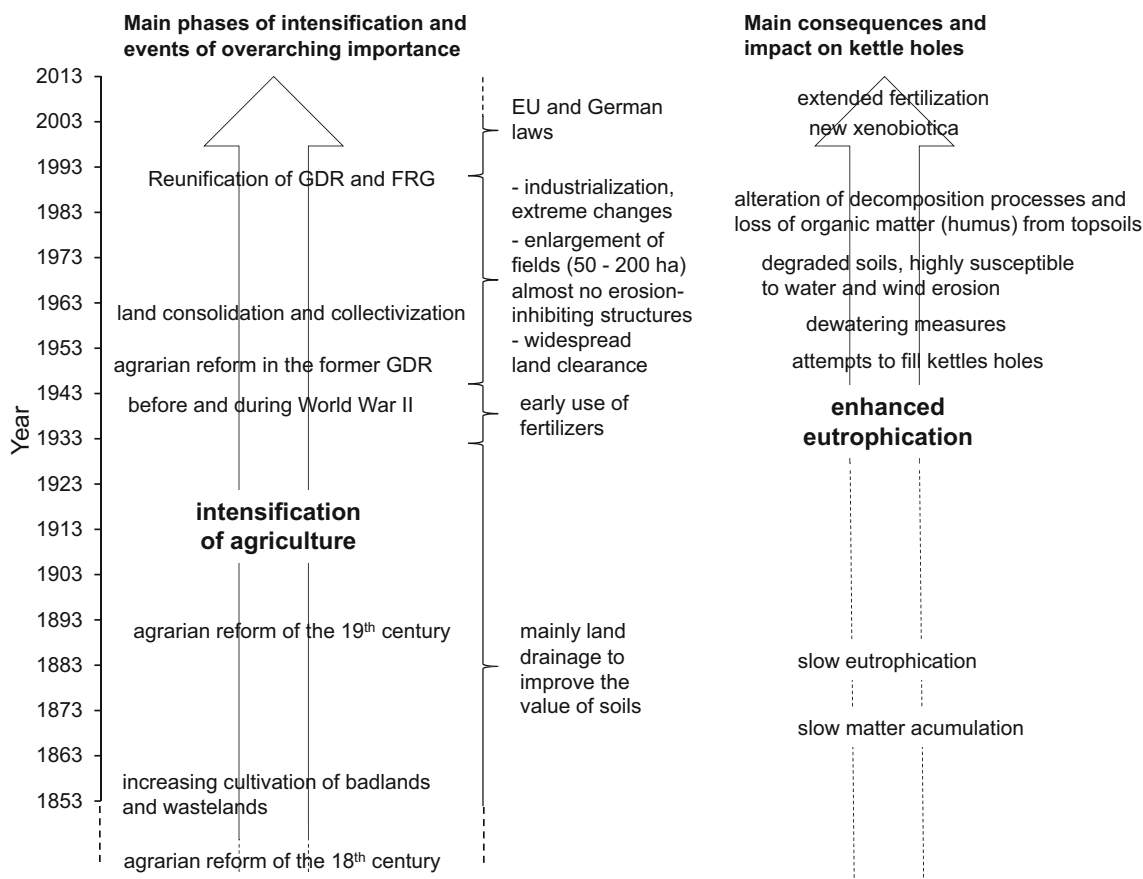
Fig. 9 Conceptual model of the main phases of land use changes and events in the Uckermark, NE Germany, and their main consequences as well as impact on the kettle holes in the area

their catchments, both before and after the 1940s (Fig. 9). Given the intensification of agriculture, documented cultural eutrophication at the RG and KR kettle holes is not surprising. An increase in SAR, nutrient accumulation and degradation of water quality is unfortunately common in many bodies of water, including kettle holes, worldwide (Engstrom et al. 2006; Preston et al. 2013). In addition to the temporally coherent trends in sediment OM, P, N and others, which together reflect a shift towards nutrient enrichment of the kettle holes over the last century, there was a distinct phase of erosion in KR. Thus, it is reasonable to assume that other morphologically similar kettle holes in the Uckermark or other areas of NE Germany, which are prone to erosion, were similarly impacted.

The increasing P input to both kettle holes was accompanied by a proportional higher input of its main binding partner Fe. Thus, the Fe/P ratio remained constant, indicating a similar P mobility. However, the kettle hole-specific differences in productivity and plant community obviously contributed to a decrease of the amount of Fe available for P binding, as indicated by a higher S/Fe ratio ($RG_1 > KR_1$), an obviously plant-mediated feedback mechanism worth studying for different plant communities in other kettle holes.

Conclusions

Kettle holes RG and KR lie in isolated, large and intensively used fields. Thus, their sediment archives preserve an excellent record of historical intensification of agriculture in their catchments. Trends in sediment nutrient composition indicate a shift towards eutrophication in both kettle holes but with differences in timing and magnitude.

Although past and recent sediments are uncontaminated to moderately contaminated by heavy metals, pulsed losses from the catchment are reflected in their stratigraphy. Temporal variability in metal inputs is attributed primarily to local variations in soil erosion and sediment yields and, to a far lesser extent, spatial variations in fertilizer application. Despite the different mineralogical composition and use of the soils at the two sites, identical geochemical processes prevailed at both kettle holes but not to the same extent. Because of the differences between the two kettle holes studied (e.g. with respect to biogeochemistry and exposure to erosion), more studies of individual basins are necessary, and little can be concluded about the spatial variability of sediment and nutrient delivery on a regional scale.

Nevertheless, qualitative environmental reconstructions for RG and KR indicate that in the past, the systems were far less P-rich and productive, with less frequent algal blooms and greater water clarity than today. Macrophyte abundance and community composition, which obviously also changed, support our findings. RG and KR illustrate that a holistic approach, which examines kettle hole responses to changes in P loading on different time scales, i.e. in the past and present, is required to ascertain the full extent of eutrophication and evaluate the potential to restore nutrient-enriched kettle holes. Other kettle holes in NE Germany that are prone to erosion could have been similarly impacted by agriculture but may differ in the extent of sediment infilling and degradation of their ecological functions.

References

Altenfelder S, Raabe U, Albrecht H (2014) Effects of water regime and agricultural land use on diversity and species composition of vascular plants inhabiting temporary ponds in northeastern Germany. Tuexenia 34:145–162. doi:10.14471/2014.34.013

Andersen JM (1976) An ignition method for determination of total phosphorus in lake sediments. Water Res 10:329–331. doi:10.1016/0043-1354(76)90175-5

Appleby P, Oldfield F (1978) The calculation of 210 Pb dates assuming a constant rate of supply of unsupported 210 Pb to the sediment. Catena 5:1–8

Bayerl G (2006) Geschichte der Landnutzung in der Region Barnim-Uckermark. – Berlin Brandenburgische Akademie der Wissenschaft (ed): Materialien der Interdisziplinären Arbeitsgruppe Zukunftsorientierte Nutzung ländlicher Räume – Land Innovation Nr. 12., Berlin. (In German)

Battarbee RW, Anderson NJ, Jeppesen E, Leavitt PR (2005) Combining palaeolimnological and limnological approaches in assessing lake ecosystem response to nutrient reduction. Freshw Biol 50:1772–1780. doi:10.1111/j.1365-2427.2005.01427.x

BB RL-EvB (2001) Brandenburgische Richtlinie-Anforderungen an die Entsorgung von Baggergut. Amtsblatt für Brandenburg 12(33), Potsdam 15.08.2001: 566–583. (In German)

Begy R, Cosma C, Horvath Z (2009) Sediment accumulation rate in the red lake (Romania) determined by Pb-210 and Cs-137 radioisotopes. Rom J Phys 54:943–949, ISSN: 1221-146X

Berger G, Pfeffer H, Kalettka T (eds) (2011) Amphibienschutz in kleingewässerreichen Ackerbaugebieten (conservation of amphibians in pond rich arable regions). Natur & Text, Rangsdorf, 384 pp (In German). ISBN 978-3-942062-02-2

Biddanda BA, Cotner JB (2002) Love handles in aquatic ecosystems: the role of dissolved organic carbon drawdown, resuspended sediments, and terrigenous inputs in the carbon balance of Lake Michigan. Ecosystems 5:431–445. doi:10.1007/s10021-002-0163-z

Bilotta GS, Brazier RE, Haygarth PM (2007) Processes affecting transfer of sediment and colloids, with associated phosphorus, from intensively farmed grasslands: erosion. Hydrol Process 21:135–139. doi:10.1002/hyp.6600

Binford MW (1990) Calculation and uncertainty analysis of 210Pb dates for PIRLA project lake sediment cores. J Paleolimnol 3:253–267. doi:10.1007/BF00219461

Brenner M, Binford MW (1988) Relationships between concentrations of sedimentary variables and trophic state in Florida lakes. Can J Fish Aquat Sci 45:294–300, ISSN: 0706-652X

Carignan R, Planas D, Vis C (2000) Planktonic production and respiration in oligotrophic shield lakes. Limnol Oceanogr 45:189–199, ISSN: 0024–3590

Croudace IW, Rindby A, Rothwell RG (2006) ITRAX. Description and evaluation of a new X-ray core scanner. In: Rothwell R G (ed), New techniques in sediment core analysis, 267. Geological Society (Spec. Public.), London, pp. 51–63

DIN ISO 18589–3 (2014) Measurement of radioactivity in the environment–soil-part 3: measurement of gamma-emitting radionuclides, 2014–02. (In German)

Donner R, Witt A (2006) Characterisation of long-term climate change by dimension estimates of multivariate palaeoclimatic proxy data. Nonlinear Process Geophys 13:485–497, www.nonlin-processes-geophys.net/13/485/2006

Engstrom DR, Schottler SP, Leavitt PR, Havens KE (2006) A reevaluation of the cultural eutrophication of Lake Okeechobee using multiproxy sediment records. Ecol Appl 16:1194–1206. doi:10.1890/1051-0761(2006)016[1194:AROTCE]2.0.CO;2

Frielinghaus M, Vahrson W-M (1998) Soil translocation by water erosion from agricultural cropland into wet depressions (morainic kettle holes). Soil Tillage Res 46:23–30. doi:10.1016/S0167-1987(98)80104-9

Gąsiorowski M (2008) Deposition rate of lakes sediments under different alternative stable states. Geochronometria 32:29–35. doi:10.2478/v10003-008-0020-y

GeoBasis (2014) GeoBasis-DE/LGB, MIL Brandenburg, 6 July 2014, (http://luaplims01.brandenburg.de/invekos_internet/viewer.htm)

Gołdyn B, Bernard R, Czyz MJ, Jankowiak A (2012) Diversity and conservation status of large branchiopods (Crustacea) in ponds of western Poland. Limnologica 42:264–270. doi:10.1016/j.limno.2012.08.006

Gołdyn B, Chudzińska M, Barałkiewicz D, Celewicz-Gołdyn S (2015) Heavy metal concentrations in the sediments of astatic ponds: influence of geomorphology, hydroperiod, water chemistry and vegetation. Ecotoxicol Environ Saf 118:103–111. doi:10.1016/j.ecoenv.2015.04.016

Guhl M, Marquardt M (2009) Einfluss einer Kalium- und Magnesiumdüngung zu Mais, auf Wachstum und Ertrag unter Wasserstress (Feldversuch). Bachelor Thesis, Hochschule Neubrandenburg, 99 pp. (In German)

Håkanson L (2005) The importance of lake morphometry and catchment characteristics in limnology–ranking based on statistical analyses. Hydrobiologia 541:117–137. doi:10.1007/sl0750-004-5032-7

Havens KE, Jin K-R, Iricanin N, James RT (2007) Phosphorus dynamics at multiple time scales in the pelagic zone of a large shallow lake in Florida, USA. Hydrobiologia 581:25–42. doi:10.1007/s10750-006-0502-8

Hermanns Y-M, Biester H (2013) A 17,300-year record of mercury accumulation in a pristine lake in southern Chile. J Palaeolimnology 49(4):547–556. doi:10.1007/s10933-012-9668-4

Jolliffe IT (2002) Principal component analysis. Springer series in statistics. Springer, New York, 489 pp

Kalettka T, Rudat C (2006) Hydrogeomorphic types of glacially created kettle holes in North-East Germany. Limnologica 36:54–64. doi:10.1016/j.limno.2005.11.001

Kalettka T, Rudat C, Quast J (2001) 18 "Potholes" in Northeast German agro-landscapes: functions, land use impacts, and protection strategies. In: Tenhunen JD, Lenz R, Hentschel R (eds) Ecosystem approaches to landscape management in central Europe, ecological studies 147. Springer, Berlin, pp 291–298

Kamiński R, Wolnicki J, Sikorska J (2011) Physical and chemical water properties in water bodies inhabited by the endangered lake minnow *Eupallasella percnurus* (Pall.), in central Poland. Arch Pol Fish 19:153–159. doi:10.2478/v10086-011-0019-2

Karasiewicz MT, Hulisz P, Noryśkiewicz AM, Krześlak I, Switoniak M (2014) The record of hydrodynamic changes in the sediments of a kettle-hole in a young glacial landscape (north central Poland). Quat Int 328–329:264–276. doi:10.1016/j.quaint.2013.09.045

Kleeberg A, Herzog C, Jordan S, Hupfer M (2010) What drives the evolution of the sedimentary phosphorus cycle? Limnologica 40:102–113. doi:10.1016/j.limno.2009.11.001

Kleeberg A, Neyen M, Kalettka T (2015) Element-specific downward fluxes impact the metabolism and vegetation of kettle holes. Hydrobiologia. doi:10.1007/s10750-015-2460-5

Koszinski S, Gerke HH, Hierold W, Sommer M (2013) Geophysical-based modeling of a kettle hole catchment of the morainic soil landscape. Vadose Zone J 12(4): doi:10.2136/vzj2013.02.0044

Kronvang B, Bechmann M, Lundekvam H, Behrendt H, Rubæk GH, Schoumans OF, Syversen N, Andersen HE, Hoffmann CC (2005) Phosphorus losses from agricultural areas in river basins: effects and uncertainties of targeted mitigation measures. J Environ Qual 34:2129–2144. doi:10.2134/jeq2004.0439

Lamentowicz M, Obremska M, Mitchell EAD (2008) Autogenic succession, land-use change, and climatic influences on the Holocene development of a kettle-hole mire in Northern Poland. Rev Palaeobot Palynol 151:21–40. doi:10.1016/j.revpalbo.2008.01.009

Lischeid G, Kalettka T (2012) Grasping the heterogeneity of kettle hole water quality in Northeast Germany. Hydrobiologia 689:63–77. doi:10.1007/s10750-011-0764-7

Meine L (2014) Bodenkundliche Untersuchung von Niedermooren im Quilloweinzugsgebiet (Uckermark) - Eine Degradationsanalyse anhand von Profilaufnahmen und Vergleich mit Altbefunden der Preußischen Geologischen Kartierung. Bachelor Thesis, Philipps University Marburg, 1–63. (In German)

Molot LA, Dillon PJ (1996) Storage of terrestrial carbon in boreal lake sediments and evasion to the atmosphere. Glob Biogeochem Cycles 10:483–492. doi:10.1029/96GB01666

Mortvedt JJ, Beaton JD (1995) Heavy metal and radionuclide contaminants in phosphate fertilizers. In: Tiessen H (ed) Phosphorus in the global environment: transfer, cycles and management. Wiley, New York, pp 93–106

Murphy J, Riley JP (1962) A modified single solution method for determination of phosphate in natural waters. Anal Chim Acta 27:31–36, ISSN: 0003–2670

Nehyba S, Nývlt D, Schkade U, Kirchner G, Francu E (2011) Depositional rates and dating techniques of modern deposits in the Brno reservoir (Czech Republic) during the last 70 years. J Paleolimnol 45:41–55. doi:10.1007/s10933-010-9478-5

Neyen M (2014) Depositional characteristics of glacial kettle holes at Kraatz and Rittgarten, NE Brandenburg, Germany. BSc (Bachelor of Science) thesis, University of Potsdam, 1–47

Pätzig M, Kalettka T, Glemnitz M, Berger G (2012) What governs macrophyte species richness in kettle hole types? A case study from Northeast Germany. Limnologica 42:340–354. doi:10.1016/j.limno.2012.07.004

Pienkowski P (2000) Disappearance of ponds in the younger Pleistocene landscapes of Pomerania. J Water Land Dev 4:55–68, ISSN: 1429–7426

Preston TM, Sojda RS, Gleason RA (2013) Sediment accretion rates and sediment composition in Prairie pothole wetlands under varying land use practices, Montana, United States. J Soil Water Conserv 68:199–211. doi:10.2489/jswc.68.3.199

R Core Team (2014). R: A language and environment for statistical computing. R Foundation for Statistical Computing, Vienna, Austria. URL http://www.R-project.org/

Rose NL, Morley D, Appleby PG, Battarbee RW, Alliksaar T, Guilizzoni P, Jeppesen E, Korhola A, Punning J-M (2011) Sediment accumulation rates in European lakes since AD 1850: trends, reference conditions and exceedance. J Paleolimnol 45:447–468. doi:10.1007/s10933-010-9424-6

Rothe M, Kleeberg A, Grüneberg B, Friese K, Pérez-Mayo M, Hupfer M (2015) Sedimentary S:Fe ratio indicates vivianite occurrence: a study from two contrasting freshwater systems. Plos One 10(11): e0143737. doi:10.1371/journal

Selle B, Schwientek M, Lischeid G (2013) Understanding processes governing water quality in catchments using principal component scores. J Hydrol 486:31–38. doi:10.1016/j.jhydrol.2013.01.030

Tamura H, Goto K, Yotsuyanagi T, Nagayama M (1974) Spectrophotometric determination of iron(II) with 1,10-phenanthroline in the presence of large amounts of iron(III). Talanta 21:314–318

Ulrich K-U, Paul L, Hupfer M (2000) Schadstoffgehalte in Sedimenten von Staugewässern. Wasser und Boden 52:27–32

Vahrson W-M, Frielinghaus M (1998) Bodenverlagerung durch Ackerbau in einer Jungmoränenlandschaft Nordostdeutschlands. Beiträge für Forstwirtschaft und Landschaftsökologie 32:109–114

Verstraeten G, Poesen J (2002) Using sediment deposits in small ponds to quantify sediment yield from small catchments: possibilities and limitations. Earth Surf Process Landf 27:1425–1439. doi:10.1002/esp.439

Villasenor T, Jaeger JM, Marsaglia KM, Browne GH (2015) Evaluation of the relative roles of global versus local sedimentary controls on Middle to Late Pleistocene formation of continental margin strata, Canterbury Basin, New Zealand. Sedimentology 62:1118–1148. doi:10.1111/sed.12181

Vincent WF (2009) Effects of climate change on lakes, p. 55–60. In: GE Likens (ed) Encyclopedia of inland waters. Elsevier

Wetzel RG (2001) Limnology. Academic, London, 1006 pp